PHYSICAL REVIEW A VOLUME 35, NUMBER 1 JANUARY 1, 1987

Stimulated Brillouin scattering and dynamical instabilities in a multimode cw dye laser

H. Atmanspacher and H. Scheingraber
Institut für extraterrestrische Physik, Max-Planck-Institut für Physik und Astrophysik, D-8046 Garching bei München, Federal Republic of Germany

V. M. Baev*
I. Institut für Experimentalphysik, Universität Hamburg, D-2000 Hamburg 36, Federal Republic of Germany
(Received 14 July 1986)

Stimulated Brillouin scattering in the dye jet inside a linear laser cavity has been investigated and found to be of significant importance for the dynamical behavior of multimode cw dye lasers. At high spectral power densities, it is responsible for a strong coupling of thousands of individual modes into a few mode packets, thus drastically reducing the number of actually existing degrees of freedom of the system. For a decreasing spectral power density, the mode-coupling strength due to stimulated Brillouin scattering lowers, accompanied by an increase of the number of mode packets. At low spectral power densities, additional mode-coupling mechanisms are supposed to account for a stepwise reduction of the number of independently oscillating mode packets. As an interesting application, the spectroscopic technique of intracavity optical-optical double resonance is discussed and demonstrated.

I. INTRODUCTION

In recent years, the dynamics of cw lasers has attracted considerable attention, since such systems represent perfect examples for synergetic systems[1] of relatively low complexity. Different kinds of instabilities have been reported[2] in the case of both single-mode and multimode systems. The experimental conditions in single-mode systems can be rather well controlled, thus providing a good chance to model the experimental results theoretically. In contrast, multimode systems can exhibit a huge abundancy of phenomena, which are still far away from being theoretically understood. The theoretical problems mainly arise from the fact that neither the actual number of degrees of freedom nor the coupling mechanisms among them are well known.

Particularly in the case of multimode dye lasers, some progress has been achieved concerning these problems. By means of the novel concepts of deterministic chaos in dynamical systems, very basic properties of laser systems have become available to experimental research. These properties relate to a phase-space description of the system, from which the dimension of its attractor as well as its Kolmogorov entropy can be determined and used to characterize chaotic behavior.[3] While the former quantity refers to the number of degrees of freedom needed to model the system, the latter one allows for a determination of the temporal correlation properties of the system.

As has been shown in two previous papers,[4,5] there is a strong relation between the attractor dimension, the Kolmogorov entropy, and the temporal correlation characteristics. Discontinuous changes of these properties at critical pump powers indicate dynamical instabilities in the behavior of the laser system. As another remarkable result, we obtained only a low number of degrees of freedom. This indicates only a few independently oscillating mode packets instead of thousands of individual laser modes. Hence the observations show a strong coupling of individual modes, which changes at critical pump powers.

In the present paper, we investigate the reported phenomena on a microscopic level. By means of stimulated Brillouin scattering (SBS) in the gain medium of the laser system, a mechanism is described which simultaneously explains efficient mode coupling and provides some understanding of the instabilities occurring as the pump power is varied. Moreover, SBS causes additional effects, which have already been reported: (i) asymmetric laser emission profiles with the maximum intensity shifted towards longer wavelength;[6,7] (ii) asymmetric absorption line profiles in the laser emission spectrum;[8] (iii) a red shift of the whole emission spectrum with increasing pump power;[7] and (iv) a dynamical red shift of the laser spectrum as a function of time.[6–8]

In Sec. II stimulated Brillouin scattering in the liquid gain medium of a linear laser cavity is discussed as the microscopic basis for the macroscopic behavior of the system. In particular, quantitative estimates are given for the frequency and the intensity of the backscattered Stokes-shifted components.

In addition to the phenomena concerning the spectral profile of the laser emission, SBS has been shown[8] to account for strong intensity fluctuations in individual modes. This type of fluctuation is briefly reviewed in Sec. III. It will be described how SBS is responsible for the behavior of the laser system at high spectral power densities.

In Sec. IV the effects provided by SBS are discussed with respect to the different features offered by the laser

emission spectrum at low spectral power densities. Some of the phenomena occurring at dynamical instabilities are explained by SBS. However, particularly the origin of the low dimensionality at low spectral power densities needs further investigation.

As an interesting application of the effects provided by SBS, the spectroscopic method of intracavity double resonance in dye lasers is discussed in Sec. V. It is shown that in the regimes of high and low spectral power densities double resonances will hardly be detectable under the present experimental conditions. By means of intracavity double resonance of H_2O it is demonstrated that the method only successfully works in an optimum power range, determined by the particular experimental parameters.

In Sec. VI, the main results are summarized.

II. STIMULATED BRILLOUIN SCATTERING IN THE GAIN MEDIUM OF A LINEAR LASER CAVITY

It is well known that an intense electromagnetic field produces density variations in the medium of propagation. Such density variations can be described by phonons, which represent scattering centers for the photons passing the medium. Stimulated scattering of photons by phonons occurs if the phonons are created by the photons which are in turn scattered. An adequate introduction into stimulated scattering processes of light by phonons has been given, e.g., by Kaiser and Maier.[9] Among the different kinds of stimulated scattering (Raman, Rayleigh, Brillouin), stimulated Brillouin scattering (SBS) represents the most efficient scattering process in liquid media.

As mentioned above, SBS in the liquid gain medium of a dye laser causes spatial gain inhomogeneities by means of density variations. These density variations can be described by phonons carrying a certain amount of energy. Due to SBS there is always an energy loss of the scattered photons by the amount of the phonon energy. Hence, the wavelength of the scattered light is Stokes shifted. The scattered light will be amplified as an ordinary laser mode if its wavelength fulfills the resonator condition, and if its intensity is sufficiently high to prevail spontaneous emission at the corresponding wavelength. In this case, the backscattered light constitutes a longitudinal laser mode which is strongly coupled to the original mode. This coupling concerns the phase as well as the amplitude of the particular mode. These arguments, although crude and premature, suggest a more detailed investigation of SBS as a suitable candidate for the mode-coupling mechanism in dye-laser systems.

Several problems have to be treated.

(1) Is the phonon relaxation time long enough to build up a standing phonon field in the dye? If this would be the case, one would have to consider polariton scattering instead of SBS, since the photon field and the phonon field would couple to a polariton field in the dye.

(2) Is the backscattered light due to SBS Stokes shifted or anti-Stokes shifted? This question is nontrivial since there is a standing-wave field in linear cavity configurations. If the phonon relaxation time is very short, the created phonons can be assumed to be in thermal equilibrium. As it will be discussed below, this situation would give rise to a predominance of Stokes-shifted light.

(3) Is the resonator condition fulfilled? This question requires an estimate of the amounts of frequency shift and linewidth of the backscattered light.

(4) Is the backscattered light sufficiently intense to constitute a longitudinal mode? In order to clear up this point, the intensity of the scattered light has to be compared with the contribution of spontaneous emission.

With respect to (1), we have to compare the thickness of the dye jet with the distance a phonon runs through during its lifetime. Since the dye solution consists of a 1:20 mixture of methanol and ethylene glycol, a good estimate should result from the data for pure ethylene glycol. The propagation velocity of phonons (sound velocity) is then $v=1.66\times10^5$ cm/sec.[10] For a typical phonon lifetime of 1 nsec,[9] a phonon reaching distance of 1.8 μm is obtained. On the other hand, the thickness of the dye jet is of the order of 350 μm. The difference of 2 orders of magnitude is large enough to exclude the formation of a standing phonon field in the dye jet. Hence, we need not treat the complicated situation of a photon-phonon coupling which gives rise to polariton scattering. Indeed, it is sufficient to account for SBS in the dye jet.

The above-mentioned problem (2) is directly connected with (1). In the case of a short phonon relaxation time, the created phonons are quickly thermalized. Then their energy distribution can be assumed to be given by a Boltzmann distribution:

$$N_f \propto N_0 \exp\left[-\frac{hf}{k_B T}\right] . \tag{1}$$

Here N_f is the number of phonons with frequency f [see Eq. (5) below] and N_0 is the total number of phonons in their ground state. Now, one can simply consider the SBS processes between longitudinal modes $j-1$, j, and $j+1$, ordered from long to short wavelengths and spaced by the frequency f. Assuming steady state for the SBS process,[9] the photon flux into mode j is given by

$$J_+ \propto M_j M_{j+1} N_0 + M_j M_{j-1} N_0 \exp\left[-\frac{hf}{k_B T}\right] . \tag{2}$$

M is the number of photons in the indexed mode. The first (second) term in Eq. (2) gives the Stokes (anti-Stokes) contribution to the photon increase in mode j.

Equivalently, the photon flux rate out of mode j is

$$J_- \propto -M_j M_{j-1} N_0 - M_j M_{j+1} N_0 \exp\left[-\frac{hf}{k_B T}\right] . \tag{3}$$

The total photon flux with respect to mode j can be approximated by

$$J = J_+ + J_- \propto M_j N_0 \frac{hf}{k_B T}(M_{j+1} - M_{j-1}) . \tag{4}$$

This means that there is always a positive photon flux in mode j from the blue side (mode $j+1$) to the red side (mode $j-1$). This situation clearly reflects the predominance of Stokes-shifted light due to SBS.

As a consequence, one should observe an asymmetric broadband laser emission spectrum with slightly favored modes towards longer wavelengths. Laser emission profiles showing this feature have already been observed and investigated.[6,7] In Fig. 1, such a profile is shown for experimental conditions described in the figure caption. The predicted asymmetry can clearly be recognized concerning the total emission spectrum as well as the particular absorption lines.

In order to explain this asymmetry by means of different possible mechanisms, one might think of the wavelength dependence of the Einstein B coefficient. However, the increase of the B coefficient towards longer wavelengths has to be compared with the losses introduced by the resonator transmission curve. Since the maximum intensity of the observed asymmetric emission profile is red-shifted, we are interested in the long-wavelength wing of a symmetric profile. Here the losses increase for longer wavelengths. With respect to a spectral distance of 5 GHz, the relative increase of the B coefficient amounts to 10^{-5}, whereas the relative increase of the losses is of the order of 10^{-4} in the case of a free-running laser system. For a cavity containing frequency-selective elements, the latter value is even larger, so that the effect of the increasing B coefficient can be completely neglected.

Another explanation for the red-shifted maximum intensity in the emission profile has been proposed recently.[7] This explanation is based on fluctuations of the refractive index of the gain medium due to local heating effects. Since the regarded process is of purely thermal character, it is equivalent to spontaneous scattering of photons by phonons. It can therefore be assumed to be of minor influence compared with stimulated processes like SBS.

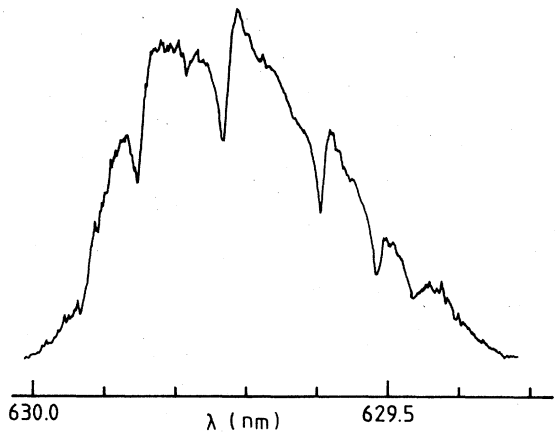

FIG. 1. Laser emission profile obtained for $P_{\text{pump}}=3.5$ W. The covered wavelength region is indicated on the horizontal scale. The spectral width is $\Delta\lambda\simeq 0.6$ nm. The appearing absorption features are due to H_2O overtone transitions and O_2 magnetic dipole transitions. A pronounced preference of the mode intensities is recognized towards longer wavelengths. The line profile of the absorption features shows an equivalent asymmetry.

For these reasons, we have clear evidence that SBS is the responsible mechanism providing the red-shift features of the laser emission spectrum, which have already been listed in the Introduction.

In order to treat the third point, the amounts of the Stokes shift and of the linewidth of the backscattered light have to be considered. The Stokes shift corresponds to the frequency f of the phonons which is given by[9]

$$f=\frac{2v\eta}{c}\ , \tag{5}$$

where v is the frequency of the incident light, $v=1.66\times 10^5$ cm/sec is the phonon velocity in ethylene glycol,[10] $\eta=1.42$ is the refractive index of ethylene glycol,[11] and c is the vacuum velocity of light. These parameters yield $f=8$ GHz, corresponding to a spectral distance which is covered by approximately 30 modes. The linewidth Δf of the backscattered light can be estimated by the inverse phonon lifetime: $\Delta f\simeq 1$ GHz. According to a longitudinal mode spacing of 250 MHz, the backscattered light extends over 4 or 5 laser modes. This means that SBS affects all oscillating longitudinal modes at a spectral distance of 15 Stokes-shift intervals. Since the total width of the laser emission ranges from 0.2 to 1 nm (25 to 125 Stokes-shift intervals), almost all modes are influenced by the scattered light. Therefore, one necessary condition for an efficient mode coupling is fulfilled.

A second condition concerns the intensity of the backscattered light, which has been addressed by point (4) above. It can be estimated by the SBS gain factor g. Typically, g is of the order of 10^{-2} cm/MW.[9] For low intracavity intensities of 200 mW, and for a spectral width of $\Delta\lambda=0.2$ nm, the laser emission contains about 720 individual modes. With an average power of 0.2/720 W per mode, with a focal radius in the dye jet of $r=25$ μm,[12] and with a jet thickness of $d=350$ μm,[12] we obtain a value of $g\simeq 5\times 10^{-9}$. In the relevant wavelength region, a power of 0.2 W is equivalent to 6×10^{17} photons per second. This value corresponds to approximately 8×10^{14} photons per second and laser mode. With the above SBS gain factor of 5×10^{-9}, a stimulated scattering of 4×10^6 Stokes-shifted photons per second and mode results near the laser threshold. This number of SBS photons has to be compared with the number of photons produced by spontaneous emission into one mode. In agreement with numerical results from a simple rate-equation approach, a number of some 10^4 spontaneous photons per second and mode is obtained. Hence, already at laser threshold a clear predominance of SBS photons over spontaneously emitted photons is revealed. According to the quadratic dependence of SBS on the intensity, this predominance even increases as a function of intracavity power.

In Secs. III and IV, we intend to discuss how the dynamical behavior of the laser system in different ranges of the spectral power density is related to SBS. To this end, we recapitulate the main effects arising from SBS in the gain medium of a linear multimode dye laser.

(i) SBS produces considerable gain inhomogeneities, since phonons are created dependent on the intensity of the electromagnetic radiation field.

(ii) The fast relaxation of the phonons is responsible for

a pronounced occurrence of stimulated Stokes-shifted backscattering. This argument agrees with the experimental observation of spectral asymmetries and dynamical redshifts of the laser emission.

(iii) Quantitative estimates reveal that SBS represents a reasonable mechanism of strong mode coupling. It can therefore be made responsible for the build-up of packets of coupled modes.

III. EFFECTS OF SBS AT HIGH SPECTRAL POWER DENSITIES

The influence of SBS on the dynamical behavior of multimode cw dye lasers increases as a function of increasing power. Therefore, the effects provided by SBS should appear most clearly in the regime of high spectral power densities. In this section we discuss the following two main effects together with their consequences.

(1) Decreasing mode correlation time with increasing spectral power density.

(2) Increasing mode-coupling strength with increasing spectral power density.

For a detailed study of the first point, we refer to the paper of Ajvasjan *et al.*[8] This paper contains the formulation of a rate equation for the photon number per mode j, accounting for intensity fluctuations due to nonlinear mode interaction caused by SBS. This equation is given by

$$\frac{dM_j}{dt} = -\gamma M_j + \beta(M_j+1) + CM_j(M_{j-1}-M_{j+1}) + F_j(t) \ . \tag{6}$$

The first two terms on the right-hand side of Eq. (6) are commonly used and describe cavity damping ($-\gamma M_j$) as well as spontaneous and stimulated emission into mode j. In detail, γ denotes the inverse photon lifetime in the cavity, and β gives the net gain coefficient of the entire laser system (including frequency-selective and -unselective losses).

The third term describes the net photon flux with respect to mode j resulting from nonlinear mode interaction according to Eq. (4). The interaction strength is given by the coefficient C:

$$C = N_0 \frac{hf}{k_B T} \tag{7}$$

with

$$N_0 \approx \frac{v}{V} \frac{(2\pi)^3 c^2}{k^2 n^2 V} \sigma_j \frac{2}{\pi\alpha} \ . \tag{8}$$

Equation (8) estimates the number N_0 of phonons in the ground state. v/V is the active gain medium v normalized with respect to the effective volume V containing the modes; k is the wave vector of the laser modes in the gain medium, n is the refractive index of the gain medium, σ_j is the Brillouin scattering cross section of mode j in the gain medium, and α is the inverse phonon relaxation time.

The last term of Eq. (6) represents the Langevin forces $F_j(t)$ simulating quantum fluctuations. They are normalized using the conditions

$$\langle F_j(t) \rangle = 0 \ , \tag{9}$$

$$\langle F_j(t) F_k(t') \rangle = \gamma \langle M_j \rangle \delta(t-t') \delta_{jk} \ . \tag{10}$$

From the numerical integration of the rate equation (6), the following facts have been derived[8] and found to be in agreement with experimental results.

(i) The amplitude of the fluctuations due to nonlinear mode interactions is of the order of magnitude of the mode intensity.

(ii) The fluctuation period decreases with increasing intensity:

$$t_{\mathrm{SBS}} \propto (C\langle M_j \rangle)^{-1} \ . \tag{11}$$

(iii) The mode correlation time t_{mode} is determined by the period t_{SBS} of fluctuations due to SBS. Quantum statistical fluctuations are of negligible influence on the mode correlation time at elevated spectral power densities. This fact must be emphasized since it modifies the interpretation of t_{mode}, as has been discussed in Refs. 4 and 5.

According to the above arguments, SBS must be realized to be responsible for the decreasing mode correlation times with increasing spectral power density. On the other hand, the quantitative estimates given in Sec. II revealed that SBS provides an efficient mechanism for coupling processes between different individual modes. Since the effects caused by SBS are enhanced by an increase of the mode intensity, we except that this mode coupling is most efficient at high spectral power densities.

As we shall show subsequently, this strong mode coupling is consistent with recent experimental results on the dynamical behavior of multimode cw dye lasers.[4,5] These results have been obtained by an investigation of the laser system in terms of its attractor in phase space. From an analysis of the geometry of this attractor, it is possible to extract the minimum number n of variables needed to model the system.

For high spectral power densities, a value of $n=3$ has been determined.[5] At first view, this number of degrees of freedom seems to be intriguingly low. Since there are actually some thousands of individual modes oscillating, the existence of only three independent variables of the system indicates a very high degree of mode coupling (possibly even complete mode locking).

Such an intense mode-coupling mechanism is provided by means of SBS. Concerning the regime of high spectral power density, we have thus indeed found a microscopic description of the low-dimensional behavior of the system.

As an alternative mechanism giving rise to mode coupling, spatial hole-burning effects have in principle to be thought of. However, under the present experimental situation in a dye jet laser, spatial hole burning is not considered to provide remarkable contributions. A quantitative estimate dealing with this problem has been given elsewhere.[13]

The investigation of the attractor describing the behavior of the laser system at high spectral power densities $P/\Delta\lambda$ has been carried out at $P/\Delta\lambda = 515$ mW/nm.[5] Lowering the spectral power density causes an increase of

the number n of variables: for instance, at 210 mW/nm a value $n=5$ has been obtained. This behavior corresponds to an increase of independently oscillating mode packets. Hence, it is consistent with a decreasing efficiency of SBS as the mechanism responsible for mode coupling.

A further decrease of $P/\Delta\lambda$ below 210 mW/nm leads into the region of low spectral power densities, where dynamical instabilities have been observed.[4,5] We treat the behavior of the system within this regime in Sec. IV.

IV. SBS AND INSTABILITIES AT LOW SPECTRAL POWER DENSITIES

In the preceding section, major progress has been achieved concerning the interpretation of the behavior of the investigated laser system at high spectral power densities. The coupling among individual modes has been understood by means of SBS processes. Now we intend to discuss SBS in relation to the dynamical characteristics of the laser emission at low spectral power densities. Because of the observed instabilities, this regime is of special interest.

Of course, our microscopic description must be consistent with recent experimental results. Therefore, we start with a brief summary of these results[4,5] as far as they are important for the present paper. In the next step, we investigate whether the observed phenomena can be explained by SBS. Finally, we shall predict additional effects which should occur if the given description is correct. These effects cause different kinds of spectral shifts of the laser emission spectrum. They will be experimentally investigated.

The analyses carried out recently[4,5] revealed the following important facts.

(1) The noninteger dimensionality D of the attractor of the investigated system in phase space changed discontinuously at $(P/\Delta\lambda)_{\text{crit}}$. This dimensionality serves as an indicator for the minimum number of variables n (degrees of freedom) needed to model the temporal evolution of the system. Starting with $n=3$ just beyond the lasing threshold, the first observed value of $(P/\Delta\lambda)_{\text{crit}}$ leads to a new attractor with $n=4$. Beyond a second instability, an attractor with $n=5$ emerges (cf. Fig. 6 in Ref. 5). This behavior is characteristic for the range of relatively low spectral power densities. The investigations cover the range between the lasing threshold and $P/\Delta\lambda=210$ mW/nm. Similar to the situation at high spectral power densities, there is only a very small number of independently oscillating mode packets, each one consisting of several hundred individual longitudinal modes. Similar results have recently been obtained by Raymer *et al.*[14]

(2) An investigation of $P/\Delta\lambda$ as a function of the pump power P_{pump} yields the dependence of the averaged mode amplitude on the control parameter of the system [cf. Fig. 5(b) in Ref. 4]. It turned out that the critical values $(P/\Delta\lambda)_{\text{crit}}$ correspond to a region of P_{pump}, where $P/\Delta\lambda$ does not significantly change. This behavior results from the fact that the increase of P is caused by an increase of $\Delta\lambda$, thus providing the constancy of $P/\Delta\lambda$. In contrast, an increasing $P/\Delta\lambda$ as a function of P_{pump} results from an increase of the intensities of already existing modes without any spectral broadening of the total laser emission. For these reasons, the representation of D as a function of $P/\Delta\lambda$ is not completely equivalent with a representation as a function of P_{pump}. In order to get a more detailed description of the instabilities providing a changing attractor of the system, the latter representation has to be considered. It clearly reveals that the transition from increasing $P/\Delta\lambda$ to constant $P/\Delta\lambda$ does not alter D. It is exactly the transition from constant to increasing $P/\Delta\lambda$ where the change of the attractor occurs.

The reported observations (1) and (2) are shown in Fig. 2, which schematically summarizes Figs. 6 and 7 of Ref. 5 and Fig. 5(b) of Ref. 4. In Fig. 2(a), $P/\Delta\lambda$ is given as a function of P_{pump}. The discontinuous changes of the slope at P_1 and P_2 indicate instabilities analogous to thermodynamical phase transitions of second order. The range between P_1 and P_2 corresponds to $(P/\Delta\lambda)_{\text{crit}}$. Figure 2(b) shows the discontinuous increase of D occurring at P_2. Although including the discontinuous behavior of D at $(P/\Delta\lambda)_{\text{crit}}$, this representation contains additional information with respect to the critical pump powers P_1 and P_2.

The complex dynamical behavior of the laser system has been interpreted by means of two nested feedback loops, connecting the physical quantities which are responsible for the evolution of the system. Figure 2 in Ref. 4 visualizes these feedback loops. Of course, the corre-

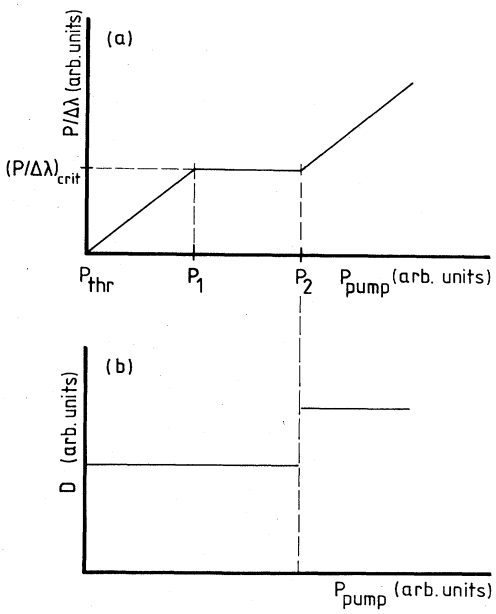

FIG. 2. Schematic illustration of the results (1)—(2) described in Sec. IV. (a) Spectral power density $P/\Delta\lambda$ as a function of pump power P_{pump}, both given in arbitrary units. At P_1 and P_2, the slope of the line changes discontinuously. Between these pump powers, the spectral power density equals $(P/\Delta\lambda)_{\text{crit}}$. (b) Attractor dimension D as a function of P_{pump} (in arbitrary units). D increases discontinuously at P_2, thus indicating the transition from one chaotic attractor to another. Note that D is not influenced at P_1.

sponding interpretation is still on a phenomenological level. However, already on this level there remains an essential question concerning the physical mechanism which couples thousands of modes into only a few independently oscillating mode packets. Within the regime of high spectral power densities, a suitable mechanism of this kind has been described in Sec. III. The efficient mode-coupling effects provided by SBS have been found to be responsible for the low dimensionality of the system.

If the spectral power density is reduced down to lower values, the number n of variables (i.e., the dimensionality of the system) increases. The corresponding increase of the number of independent mode packets agrees with the fact that SBS effects should severely reduce with decreasing mode intensity. Hence, at low intensities we would expect a rather high dimensionality of the system, if its behavior was governed by SBS processes.

This prediction contradicts the experimental observation of low dimensionalities at low spectral power densities. Thus we have to conjecture that there must be additional mode-coupling phenomena which drastically gain influence at low spectral power densities. The underlying mechanisms might be some kind of parametric processes. Experimental and theoretical work on this subject is in progress. In this context, the processes described by Hillman *et al.*[15] could be of significant importance.

Although SBS can obviously not be the reason for the low dimensionality at low spectral power densities, it should be possible to observe asymmetries and red-shift effects even in the low-power regime. This can be concluded from the estimated predominance of SBS light compared with spontaneously emitted photons in the gain medium. According to point (4) of Sec. II, even just above the lasing threshold effects of SBS become nonnegligible.

Indeed, the influence of SBS at low spectral power densities can experimentally be recognized by a red shift of the laser emission. Moreover, the character of the spectral shift changes according to the critical values of $P/\Delta\lambda$, i.e, at the dynamical instabilities. The following details have been observed.

An increase of P_{pump} towards P_1 (cf. Fig. 2) provides the described features of increasing spectral power density and constant D. In this range the laser emission spectrum shows a pronounced increase of the mode intensities, while the spectral width $\Delta\lambda$ (corresponding to the number of modes) only modestly grows. Since the SBS gain factor grows with increasing mode intensity, a slight red shift of the whole asymmetric emission spectrum of the laser results as P_{pump} is increased. This behavior is clearly visible in Fig. 3, showing the red and blue limit of the emission spectrum as a function of P_{pump}. The indicated error bars show the statistical deviation of five subsequent measurements per each value of P_{pump}. The wavelength limits of the laser emission spectrum have been determined according to 1% of the maximum emission. Because of the prominent absorption features in the spectrum, the commonly used full width at half maximum (FWHM) would provide ambiguous results.

At P_1, a first type of instability occurs. It does not affect D, so that the attractor of the system is not altered.

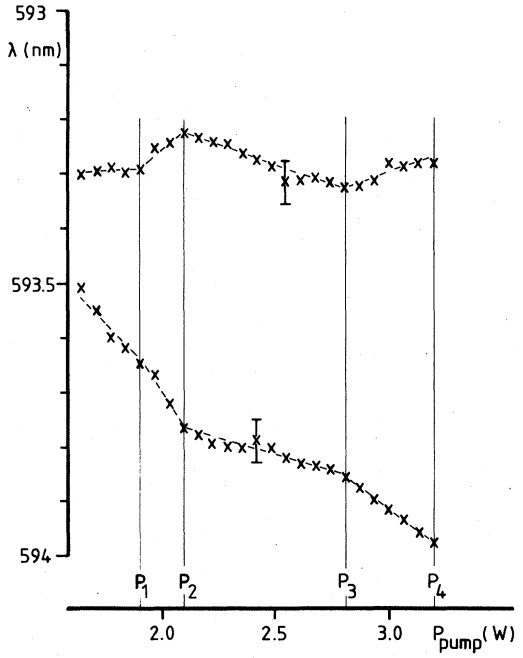

FIG. 3. Upper and lower wavelength bounds of the laser emission spectrum as a function of pump power P_{pump}. The bounds have been determined according to 1% of the maximum intensity of the emission spectrum. Typical errors are indicated. At the same values of P_1 and P_2 as in Fig. 2, distinct changes in the broadening behavior of the emission profile are observed. Moreover, these changes occur again at P_3 and P_4.

However, there is a distinct change of the slope of $P/\Delta\lambda$ versus P_{pump}. This bend arises because of a change in the behavior of the laser emission spectrum. The mode intensity does no longer increase, but the onset of a spectral broadening is observed. The mode intensity seems to be "saturated" in the sense that it becomes easier for the system to use any additional pump power for an increase of $\Delta\lambda$, i.e., for a creation of additional modes. Such a "saturation" effect only makes sense if there is a strong phase coupling among the individual modes. In this case, only a small amount of the totally available gain is used for the amplification of already existing modes.

The spectral broadening of the laser emission beyond P_1 extends approximately symmetrically towards longer and shorter wavelengths (cf. Fig. 3). Since the mode intensity in the center of the emission spectrum does not considerably increase between P_1 and P_2, we do not observe a red shift as between P_{thr} and P_1. In this region, the number of variables given by D is not enhanced. On the other hand, the number of individual modes increases steadily. It can already now be presumed that there will be a certain pump power at which the mode-coupling mechanism will no longer be strong enough to prevent the formation of an additional mode packet.

This is exactly what happens at P_2. The additional mode packet will show a phase shift with respect to the other ones, thus being able to profit from formerly unused

gain. The instability occurring at P_2 drives the system into a new (chaotic) attractor, corresponding to an increase of the number of degrees of freedom. At the same point, the slope of $P/\Delta\lambda$ vs P_{pump} changes again. The spectral broadening stops, since a more "economic" use of the gain has emerged due to one more mode packet. Hence, the mode intensity again starts to increase. As a function of P_{pump}, we observe a slight red shift of the whole laser emission spectrum equivalent to the range below P_1 (cf. Fig. 3).

It has to be pointed out that the critical values of P_{pump} are not reliably reproducible. Also, the particular slopes between successive critical values of P_{pump} are not quantitatively reproduced. However, the discussed qualitative behavior of the emission spectrum as a function of P_{pump} is generally observed. Furthermore, the various red-shift phenomena do not depend on the spectral position of the laser emission with respect to the fluorescence maximum of the dye. This fact excludes a dominant influence of the gain coefficient of the dye solution on the observed red shift of the laser emission.

V. AN APPLICATION: INTRACAVITY DOUBLE RESONANCE

Intracavity double-resonance spectroscopy has already been carried out in the spectral region from infrared to radio-frequency ranges.[16] Experimentally, CO_2 gas lasers have been commonly used in combination with a microwave or radio-frequency resonator. However, until now intracavity double resonance in the optical wavelength region has never been reported. In view of the wide-spread use of continuously tunable dye lasers covering the optical wavelength region, this seems to be rather curious. In the present section, we shall discuss why the lack of experimental success in intracavity optical-optical double resonance (OODR) is less a matter of curiosity, but has conclusive reasons in the complicated dynamical behavior of multimode dye-laser systems.

Intracavity double resonance is a highly desirable spectroscopic technique, since it combines the advantages of (i) the high sensitivity of intracavity absorption, and of (ii) the state-selective information provided by Doppler-free double-resonance methods.[17] In particular, intracavity double resonance should be useful with respect to faint transitions of polyatomic molecules. Due to various coupling mechanisms, single resonance (e.g., absorption) spectra of such molecules often show complicated and irregular line features. As a further interesting application, the analysis of gas discharge spectra of molecular ions has to be mentioned.

In principle, intracavity double resonance can be realized in the following manner. The probe which has to be investigated is placed into the cavity of a dye laser B, so that the intracavity laser beam passes the probe. The narrow-band radiation of a second laser A is used to pump a known transition in the probe. By a modulation of the radiation of laser A, the population density in the initial and in the final state of the transition is caused to vary with the frequency of the modulation. Within the broadband emission spectrum of laser B, all transitions sharing a common state with the pumped transition can then be found using a phase-sensitive detection technique.

It is easily recognized that the described method will merely work under the condition of independently oscillating, i.e. uncoupled, modes in the broadband spectrum of laser B. In the case of a strong mode coupling, the modulation of the pumped transition will be transferred to all those modes which are coupled with the directly affected modes. As a consequence, the phase-sensitive detection will simply reproduce the broadband emission spectrum of all coupled modes instead of a frequency-selective OODR spectrum.

This consideration shows the important influence of the complex mode-coupling mechanisms described in the preceding sections. Intracavity double resonance in multimode cw dye lasers will be unpracticable at very low as well as at high spectral power densities, since in these intensity ranges strong mode coupling is present. Only in the intermediate intensity range of weak mode coupling can frequency-selective double resonance be expected. This fact has to be accounted for in the experimental realization which is described in Sec. V A.

Furthermore, an additional effect must be taken into account. For an appropriate intensity region with the smallest possible degree of mode coupling, a corresponding mode correlation time t_{mode} results due to power-dependent intensity fluctuations (cf. Sec. III). It is given by t_{SBS} in Eq. (6), and characterizes the relaxation of an intracavity absorption dip if the absorption is switched off.[18] This relaxation corresponds to the "memory" of the system with respect to the preceding absorption.

As a second time scale one has to consider the period t_m of the modulation of the absorption coefficient, which is caused by the modulated intensity of laser A. In addition to t_{mode} and t_m, the characteristic rise time of the investigated absorption line in the unperturbed case ($t_{\text{mode}} \to \infty$, $t_m \to \infty$) is important. It is given by $\tau = (\kappa c)^{-1}$. After this time, the relative depth I/I_0 of the absorption dip in the laser emission spectrum amounts $1/e$ due to Beer's law. The temporal evolution of I/I_0 due to Beer's law is shown by the straight line in Fig. 4. For small absorption coefficients κ, the mode correlation time (some hundred μsec) corresponding to an optimum spectral power density is usually smaller than τ ($\tau = 3$ msec for $\kappa = 10^{-8}$ cm^{-1}).

The optimum value of the spectral power density depends on the degree of mode coupling. It is therefore determined by the experimental parameters and cannot be chosen in an arbitrary manner. For this reason we have to investigate how the OODR spectrum depends on the period t_m of the modulation. Three cases can be distinguished. We treat the absorption as a rectangular function of time with period $2t_m$. The absorption is considered to be switched on at $t = 0$.

1. $t_m \ll t_{mode}$. In this case, the relative depth I/I_0 of the absorption dip decreases due to Beer's law, until t_m is reached. At t_m, the absorption is switched off, and the intensity in the dip recovers due to the relaxation time scale t_{mode}. Thus, I/I_0 decreases until the absorption is switched on again. The temporal evolution of I/I_0 is illustrated by the dashed line in Fig. 4. The strength of the

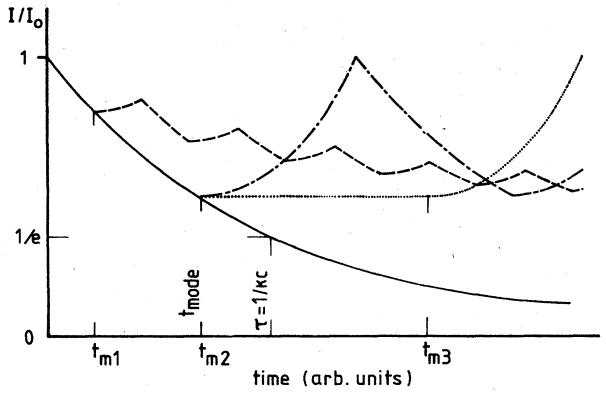

FIG. 4. Temporal dynamics of the relative depth I/I_0 of an absorption dip for the case of a modulated absorption coefficient (OODR). The straight line corresponds to an undisturbed ($t_{\text{mode}} \to \infty$) and unmodulated ($t_m \to \infty$) evolution of the absorption dip. Its relative depth I/I_0 will be $1/e$ after $\tau=(\kappa c)^{-1}$ due to Beer's law. A mode correlation time t_{mode} for usual experimental conditions is given on the horizontal axis. The nonsolid curves represent three different situations concerning the modulation period t_m: (1) $t_m \ll t_{\text{mode}}$ (dashed line); (2) $t_m \simeq t_{\text{mode}}$ (dash-dotted line); (3) $t_m > t_{\text{mode}}$ (dotted line). The optimum condition for a strong OODR signal is characterized by case (2).

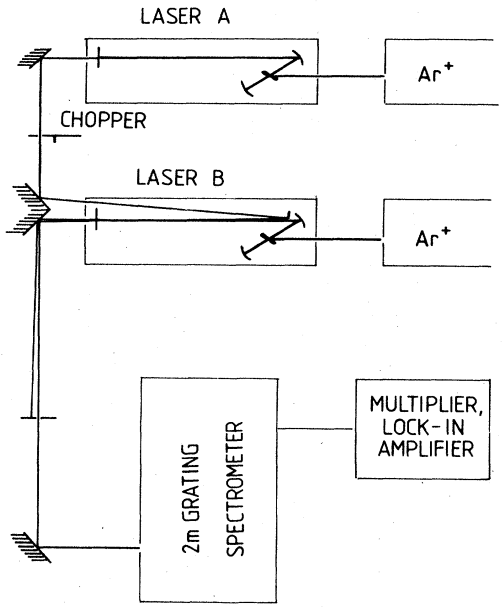

FIG. 5. Schematic illustration of the experimental arrangement for intracavity double resonance. The modulated radiation of laser A is used to pump a particular H_2O transition. Within the resonator of laser B, the spatial coincidence of both laser beams provides the transfer of this modulation to the longitudinal modes of laser B by means of the radiation interaction with the absorbing H_2O molecules.

corresponding OODR signal is given by the amplitude of I/I_0 as a function of time. This amplitude decreases with decreasing modulation period.

2. $t_m \approx t_{mode}$. Due to analogous arguments as above, this case provides an increased OODR signal, since the maximum rise time of the absorption dip is utilized by the on state of the absorption. This situation is illustrated by the dash-dotted line in Fig. 4. It yields the optimum condition for the modulation period.

3. $t_m > t_{mode}$. An increase of t_m beyond t_{mode} does not lead to a further increase of I/I_0, since the rise time of the absorption dip is limited by t_{mode}. In this situation (dotted line in Fig. 4) the OODR signal is smaller than in case 2, since high-frequency components will dominate in the output signal.

A. Experimental details

In order to demonstrate intracavity OODR, H_2O molecules have been selected as a convenient probe. The concentration of water vapor in the atmosphere is known to be sufficiently high that it can be easily detected by intracavity spectroscopy.[19,20] On the other hand, considerable collisional cross sections among energetically neighbored molecular levels are present under atmospheric pressure. Collision-induced transfer from the pump-level population into other energy levels reduces the state selectivity of the method, since it simultaneously transfers the modulation of the population density to other levels.

The experimental arrangement is schematically shown in Fig. 5. The double resonance is carried out inside the cavity of a broadband dye laser B operated with Rhodamine 6G. The covered wavelength region was tunable by means of an interference filter coated for 450 nm. As a pump laser A, a linear cw dye laser of the same type was used. The radiation emitted by laser A was tuned by a commercial birefringent filter. Its linewidth was 0.1 cm^{-1} at an output power of 800 mW.

The wavelength of laser A had to be tuned to the wavelength of the particular H_2O transition which was pumped inside the cavity of laser B. The concerning transition is given below. The modulation of the pump radiation has been provided by a mechanical chopper. The radiation of laser A is fed into the cavity of laser B near its fold mirror, thus providing the highest possible spatial overlap of both beams.

For the simplest kind of a double resonance, the pumped transition can be chosen identical with the detected transition. Hence, the broadband emission of laser B was tuned to the wavelength region around the pump wavelength. As a result, the double-resonance signal should at least show the pumped transition itself. The radiation emitted by laser B was spectrally resolved in a 2-m grating spectrometer, photoelectrically scanned, and detected by means of a lock-in amplifier. The reference frequency was given by the modulation frequency of the chopper element. The modulated radiation which also passes the outcoupling mirror of laser B is stopped before entering the spectrometer. Therefore, the lock-in amplifier will only yield a signal at those wavelengths where the longitudinal modes of laser B oscillate with the modulation frequency of the pump radiation of laser A.

In ordinary (extracavity) double resonance, this frequency merely occurs at those wavelengths which correspond to transitions radiatively (or collisionally) coupled to the pump transition. However, the intracavity arrangement introduces the additional effect of mode coupling which is of largest influence at low and at high powers. As mentioned above, mode coupling should therefore prevent useful intracavity double resonance in these power ranges. Indeed, we were not able to observe any wavelength-specific double-resonance signal in the range just beyond threshold as well as at high powers. Only an intermediate range beyond an output power of about 100 mW enabled the detection of significant double resonances.

In order to combine the capability of double-resonance detection with the requirements on the mode correlation time, laser B was operated at the lower bound of the power range where double resonance is detectable. As has been described in Sec. III, the mode correlation time decreases with increasing spectral power density due to SBS effects. However, long mode correlation times are desirable with respect to a considerable modulation amplitude of I/I_0. This modulation amplitude determines the intensity of the double-resonance signal according to a particular investigated transition.

Hence, the optimum power of laser B for intracavity double resonance is simply obtained by maximizing the intensity of the double-resonance signal. An output power of 120 mW corresponding to a spectral power density of approximately 150 mW/nm turned out to be appropriate. At this power, the spectral width of the laser profile amounts to 15 cm^{-1}. The mode correlation time at 150 mW/nm was $t_{mode} \simeq 250$ μsec. In order to realize the optimum condition $t_m \approx t_{mode}$, we used a modulation frequency of 2 kHz.

A suitable wavelength region for the experiment has been selected in order to cover the wavelengths of at least two H_2O transitions sharing a common level. Due to the identification of various optical H_2O overtone transitions given by Antipov *et al.*,[21] we selected the wavelength range around 589.2 nm. In this range, the following two lines of relatively high transition moment have been associated with the same lower level: transition I,

$$(J''=3,\tau''=-3)\rightarrow(J'=4,\tau'=-4),\ (401)\ \text{band}\ ,$$

and transition II,

$$(J''=3,\tau''=-3)\rightarrow(J'=4,\tau'=-3),\ (302)\ \text{band}\ .$$

The lower level (the quantum numbers of which are characterized by a double prime) belongs to the lowest vibrational (000) state within the electronic ground state of H_2O. Its rotational quantum number is $J''=3$. Since H_2O is an asymmetric top molecule, the splitting of the rotational levels into $2J+1$ sublevels with quantum numbers $\tau=-J,\ldots,J$ has to be regarded in addition.[22] For the given transitions, $\tau''=-3$.

The different upper levels (with quantum numbers characterized by a single prime) with given J' and τ' belong to the different vibrational bands (302) and (401), both of the electronic ground state. The corresponding wavelengths of the transitions are 589.240 nm (I) and 589.166 nm (II).

From the data given by Antipov *et al.*[21] as well as by Moore *et al.*,[23] one obtains that there is an H_2O line at 589.151 nm close to transition II. It has been identified to correspond to an $R\,4(302)$ transition, sharing no common level with either I or II. By means of intracavity absorption, this line could not be resolved from transition II, as can be seen in the upper part of Fig. 6. For this reason, we decided to pump transition I in order to obtain a double-resonance signal at the wavelength of II which should no longer be perturbed by the overlapping $R\,4(302)$ line.

B. H_2O intracavity OODR

The intracavity OODR spectrum of H_2O in the selected wavelength region is shown in the lower part of Fig. 6.

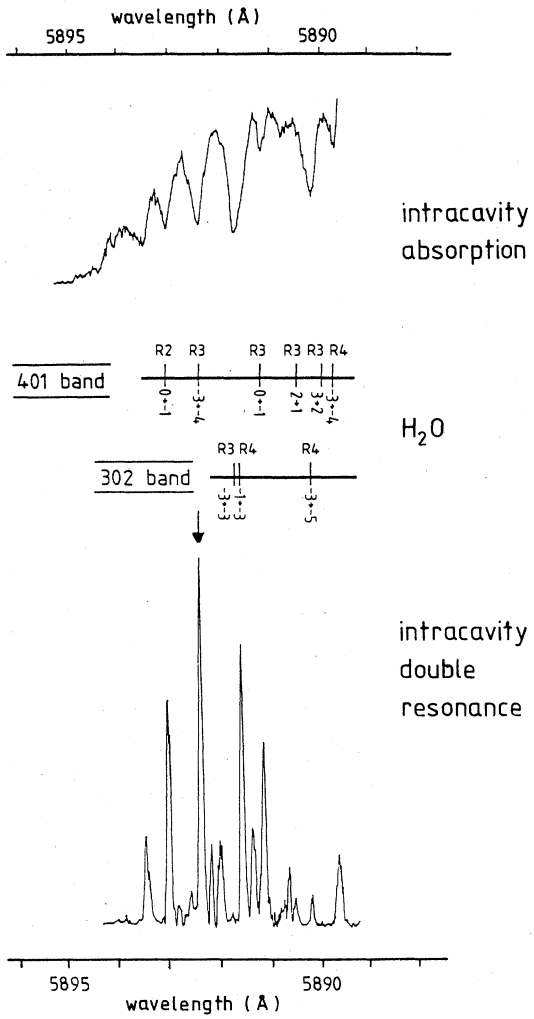

FIG. 6. Intracavity single- (above) and double-resonance spectra (below) of H_2O around 589.2 nm. The identification of the transitions due to Ref. 21 is indicated. In the double-resonance spectrum, the line marked with an arrow corresponds to the pumped transition.

For comparison, the single-resonant intracavity absorption spectrum is given in the upper part. The identification of the particular lines due to Antipov *et al.*[21] is also indicated. It is immediately recognized that the double-resonance spectrum contains clearly more and better resolved lines than obtained by intracavity absorption.

The registered OODR lines are summarized in Table I. In the first column, the measured line positions are given together with their statistical error obtained from ten subsequently recorded spectra. The second column contains the positions of the lines observed by Antipov *et al.* in the corresponding wavelength region. Their identification is given in the third column. For instance, "$R\,3(401)\ -2/-3$" denotes an $R\,3$ transition with $\tau''=-2$ and $\tau'=-3$, the upper level of which belongs to the (401) vibrational band. In the last column, those lines are marked which have also been detected by means of intracavity absorption. The strongest lines are denoted by xx.

As the most surprising result, Table I reveals that transition II yields no signal, although it represents the only transition sharing a common level with the pumped transition I due to Antipov *et al.* Most of the lines observed by Antipov *et al.* and by intracavity absorption appear in the OODR spectrum as well. In addition, nine unidentified lines can unambigously be detected.

Among the strongest lines observed by Antipov *et al.* and by intracavity absorption, only the $R\,4(302)$ line at 589.009 nm is missed in the OODR spectrum. It seems to be a strange coincidence that the line at 589.151 nm, detected instead of transition II in the OODR spectrum, also corresponds to an $R\,4(302)$ transition. For these facts, the identification of the lines at 589.166 and 589.151 nm might be incorrect. If, e.g., the quantum numbers concerned were exchanged, the problem of the missing double resonance of I and II would be resolved. Moreover, both strong $R\,4(302)$ transitions situated in the observed wavelength region would not appear in the OODR spectrum. Anyway, there are, already within the small-wavelength region investigated by means of OODR, obvious inconsistencies in the designation of the quantum numbers given by Antipov *et al.*

The double-resonant detection of all additional H_2O lines not sharing a common level with the pump line can be explained by strong collisional coupling. As mentioned above, this mechanism accounts for a transfer of the modulation of the pump level to levels which are neighbors energetically. In order to confirm the influence of collisional coupling, the pump radiation was tuned to the wavelength of transition II. Apart from variations of the particular line intensities, no further effect could be observed. In particular, no additional lines appeared.

In principle, this disadvantage could be removed by a reduction of the pressure. However, a lower pressure yields a smaller absorption coefficient. For rather faint

TABLE I. Positions of the measured OODR lines (column 1) and of the lines observed by Antipov *et al.* (Ref. 21) in the corresponding wavelength region (column 2). Wavelengths are given in nm. The designation of the quantum numbers according to the observed transitions has been taken from Antipov *et al.* (column 3). Finally, it is indicated (column 4) whether the particular transition has also been detected by means of intracavity absorption. The strongest transitions are marked by xx.

Line position double resonance (nm)	Line position Ref. 21 (nm)	Identification Ref. 21	Intracavity absorption
589.390(2)			
589.349(3)	589.351	$R\,3(401)\ -2/-3$	xx
589.303(3)	589.305	$R\,2(401)\ 0/-1$	xx
589.283(4)			
589.258(2)	589.263	$Q\,6(302)\ -5/-3$	
589.242(2)	589.240	$R\,3(401)\ -3/-4$	xx
589.221(3)			
589.210(2)			
589.199(2)			
589.174(4)			
	589.166	$R\,3(302)\ -3/-3$	xx
589.155(3)	589.151	$R\,4(302)\ -1/-3$	xx
589.134(2)			
589.113(2)	589.118	$R\,3(401)\ 0/-1$	xx
589.072(3)	589.075		x
589.061(3)	589.068		x
589.048(3)			
	589.033	$R\,3(401)\ 2/1$	
589.016(2)			
	589.009	$R\,4(302)\ -3/-5$	xx
	588.986	$R\,3(401)\ 3/2$	
588.961(2)	588.964	$R\,4(401)\ -3/-4$	xx

transitions, pressure reduction, therefore, is practically limited by the corresponding decrease of the line intensities in the OODR spectrum.

Those nine OODR lines which are found in addition to the single-resonant spectra must be interpreted due to transitions which do not originate from the (000) band. These lines can be explained by two different kinds of processes. Firstly, they could be attributed to transitions starting from the upper level of the pump transition, populating higher levels of the electronic ground state in a second absorption step. Secondly, they can be caused by stimulated emission from the pumped level down to lower levels in the (000) band.

VI. SUMMARY

The investigations reported in this paper continue our research on dynamical instabilities in a multimode cw dye laser. As an important result of previous work,[4,5] the existence of strong mode coupling in extended ranges of the intracavity spectral power density had to be concluded. However, the microscopic processes causing this mode coupling remained unclear.

As has been shown in the present paper, such a microscopic mechanism is provided by SBS occurring in the dye jet inside the laser cavity. The influence of SBS on the laser emission spectrum has been quantitatively estimated and compared with different possible competing processes. The obtained results give clear evidence that SBS plays a decisive role with respect to the dynamics of the system.

Based on this fact, a model has been developed which contains the following points.

(i) An effective coupling mechanism for individual laser modes is given by SBS. This mechanism is responsible for the low dimensionality of the system at high spectral power densities.

(ii) In contrast, the low dimensionality of the system at low spectral power densities requires an additional mode-coupling mechanism, since the coupling strength due to SBS decreases towards low intensities. The influence of parametric processes in this context is still under investigation.

(iii) Over the total power range, the additional phenomena of spectral asymmetries and shifts of the laser emission profile can be explained by SBS. Moreover, the character of the spectral shift changes at the dynamical instabilities observed at low spectral power densities.

These points reveal that the onset of the influence of SBS depends on the particular effect which is considered. While red shifts and asymmetries due to SBS occur already slightly beyond the laser threshold, mode coupling due to SBS seems to become predominant beyond some intermediate spectral power density (somewhere between 210 and 515 mW/nm for the investigated laser system).

The processes caused by SBS at different intracavity spectral power densities have been shown to be of practical relevance for the spectroscopic technique of intracavity double resonance in a multimode dye laser. The conditions determining the optimum power range and the optimum modulation frequency for intracavity double resonance have been evaluated. Finally, optical-optical intracavity double resonance of H_2O has been demonstrated.

ACKNOWLEDGMENTS

One of the authors (V.M.B.) wishes to acknowledge support from the Alexander von Humboldt Foundation. H.A. gratefully acknowledges support from the Reimar Lüst Foundation.

---

*On leave from P. N. Lebedev Physics Institute, Academy of Sciences of the U.S.S.R., Moscow 117 924, U.S.S.R.

[1]H. Haken, *Synergetics—An Introduction,* 3rd ed. (Springer, Berlin, 1983).

[2]For a review, see N. B. Abraham, L. A. Lugiato, and L. M. Narducci, J. Opt. Soc. Am. B **2**, 7 (1985).

[3]A general treatment of the underlying concepts and a description of numerical procedures yielding attractor dimension and Kolmogorov entropy has been given by J.-P. Eckmann, and D. Ruelle, Rev. Mod. Phys. **57**, 617 (1985), and references therein. These procedures have successfully been applied in completely different scientific disciplines like hydrodynamics [A. Brandstäter, J. Swift, H. L. Swinney, A. Wolf, J. D. Farmer, E. Jen, and P. J. Crutchfield, Phys. Rev. Lett. **51**, 1441 (1983)], acoustics [W. Lauterborn and J. Holzfuss, Phys. Lett. **115A**, 369 (1986)], neurophysiology [A. Babloyantz, J. M. Salazar, and C. Nicolis, Phys. Lett. **111A**, 152 (1985)], and climatology [G. Nicolis and C. Nicolis, Proc. Natl. Acad. Sci. USA **83**, 536 (1986)]. Corresponding investigations in quantum optical systems have been performed for single-mode [A. M. Albano, J. Abounadi, T. H. Chyba, C. E. Searle, S. Yong, R. S. Gioggia, and N. B. Abraham, J. Opt. Soc. Am. B **2**, 47 (1985)] and multimode lasers [H. Atmanspacher and H. Scheingraber, Phys. Rev. A **34**, 253 (1986)].

[4]H. Atmanspacher, H. Scheingraber, and C. R. Vidal, Phys. Rev. A **33**, 1052 (1986).

[5]H. Atmanspacher and H. Scheingraber, Phys. Rev. A **34**, 253 (1986).

[6]V. M. Baev, T. P. Belikova, S. A. Kovalenko, E. A. Sviridenkov, and A. F. Suchkov, Kvant. Elektron. (Moscow) **7**, 903 (1980) [Sov. J. Quant. Electron. **10**, 517 (1980)].

[7]F. Stoeckel and G. H. Atkinson, Appl. Opt. **24**, 3591 (1985).

[8]Yu. M. Ajvasjan, V. M. Baev, V. V. Ivanov, S. A. Kovalenko, E. A. Sviridenkov, Kvant. Elektron. (Moscow) (to be published).

[9]W. Kaiser and M. Maier, in *Laser Handbook,* edited by F. T. Arecchi and E. O. Schulz-Dubois (North-Holland, Amsterdam, 1972), Vol. 2.

[10]*Handbook of Chemistry and Physics,* 57th ed., edited by R. C. Weast (Chemical Rubber Company, Cleveland, 1977), p. E47.

[11]*Zahlenwerte und Funktionen aus Physik und Technik,* Vol. 2/8 of *Landolt-Börnstein,* edited by K. H. Hellwege and A.

M. Hellwege (Springer, Berlin, 1962), p. 5/610.
[12]Laser parameters due to the specification sheets of Coherent, Inc. (1980).
[13]V. M. Baev, T. P. Belikova, E. A. Sviridenkov, and A. F. Suchkov, Zh. Eksp. Teor. Fiz. **74**, 43 (1978) [Sov. Phys.—JETP **47**, 21 (1978)].
[14]M. G. Raymer, C. Radzewicz, and I. McMackin (private communication).
[15]L. W. Hillman, J. Kraszinski, K. Koch, and C. R. Stroud, Jr., J. Opt. Soc. Am. B **2**, 211 (1985).
[16]E. Arimondo and T. Oka, Phys. Rev. A **26**, 1494 (1982), and references therein.
[17]W. Demtröder, *Laser Spectroscopy* (Springer, Berlin, 1981).
[18]N. A. Raspopov, A. N. Savchenko, and E. A. Sviridenkov, Kvant. Elektron. (Moscow) **4**, 736 (1977) [Sov. J. Quant. Electron. **7**, 409 (1977)].
[19]E. N. Antonov, V. G. Koloshnikov, and V. R. Mironenko, Opt. Commun. **15**, 99 (1975).
[20]V. M. Baev, V. Ya. Gulov, E. A. Sviridenkov, and M. P. Frolov, Kvant. Elektron. (Moscow) **2**, 1328 (1975) [Sov. J. Quant. Electron. **5**, 724 (1975)].
[21]A. B. Antipov, A. D. Bykov, V. A. Kapitanov, V. P. Lopasov, Yu. B. Makushkin, V. I. Tolmachev, O. N. Ulenikov, and V. E. Zuev, J. Mol. Spectrosc. **89**, 449 (1981).
[22]G. Herzberg, *Molecular Spectra and Molecular Structure* (Van Nostrand, New York, 1951), Vol. 2.
[23]C. E. Moore, M. G. J. Minnaert, and J. Houtgast, *The Solar Spectrum 2935 Å to 8770 Å*, Natl. Bur. Stand. (U.S.) Monograph No. 61 (U.S. GPO, Washington, D.C., 1966).